

Image Cover Sheet

CLASSIFICATION UNCLASSIFIED	SYSTEM NUMBER 516302 
---	--

TITLE
Measurement of optical limiting threshold in various materials

System Number:
Patron Number:
Requester:

Notes:

DSIS Use only:
Deliver to: DK

This page is left blank

This page is left blank

UNCLASSIFIED

Measurement of Optical Limiting Threshold in Various Materials

D. Vincent
DREV

Defence Research Establishment Valcartier

Report

TR 2001-028

October 2001

SANS CLASSIFICATION

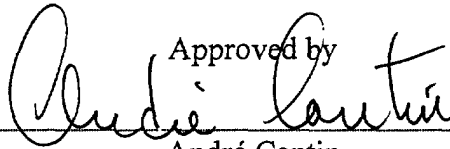
UNCLASSIFIED

Author



Denis Vincent

Approved by



André Cantin

H/EOW Section

© Her Majesty the Queen as represented by the Minister of National Defence, 2001

© Sa majesté la reine, représentée par le ministre de la Défense nationale, 2001

UNCLASSIFIED

Abstract

In the search for materials suitable for optical limiting applications to protect eyes and electro-optical sensors against laser radiation, fine carbon particles suspended in a liquid have been shown to possess highly desirable properties. This publication reports on the measurement of the threshold energy fluence for optical limiting of nanosecond and microsecond pulses in a high-performance carbon suspension named DREV CBS-100. Thresholds as low as 24 mJ/cm² (nanosecond regime) and 100 mJ/cm² (microsecond regime) have been obtained. The technique has been tested by measuring materials whose properties can be found in the technical literature.

Résumé

Les recherches sur les matériaux susceptibles de protéger les yeux et les capteurs électro-optiques contre le rayonnement laser par limitation optique ont montré que de fines particules de carbone en suspension dans un liquide présentent des caractéristiques intéressantes. Ce rapport expose les résultats des mesures du seuil d'activation de la limitation optique d'impulsions laser d'une durée de quelques nanosecondes et d'une microseconde dans une suspension de carbone très performante appelée DREV CBS-100. Les résultats montrent des seuils aussi bas que 24 mJ/cm² dans le régime nanoseconde et 100 mJ/cm² dans le régime microseconde. La technique de mesure utilisée a été vérifiée avec des matériaux dont les propriétés se retrouvent dans la littérature spécialisée.

UNCLASSIFIED

This page intentionally left blank.

UNCLASSIFIED

Executive summary

Due to the ever-increasing presence of laser sources such as rangefinders, designators and illuminators in general, some means are required to protect eyes and EO sensors against potential injuries. In an attempt to reduce the risk of eye damage in an unknown laser environment, DREV is investigating materials that could be used as limiters of laser radiation in optical sights.

In particular, a liquid suspension of fine carbon particles has been shown to exhibit useful limiting effects in the visible and near-infrared bands. To obtain the lowest transmitted laser energy level while retaining a good total luminous transmittance, it is necessary to optimize the different parameters of the suspension and, in particular, the choice of the carbon source, the surfactant and the liquid medium. An important parameter to monitor during the optimization process is the energy fluence (laser pulse energy on a unit area) required to activate a useful limiting effect: the threshold fluence. A low threshold fluence results in a low limited energy level and a better protection. This report discloses the results of measurements taken with a set of various carbon suspensions including DREV's CBS-100 which, to our knowledge, offers the best performance against short and long laser pulses at repetition rates up to 6 pps. These measurements were taken with a simple focussing optical geometry apertured to $f/20$ and using a small pinhole as an analysis aperture. The focussed laser spot inside the nonlinear material is imaged on the analysis aperture and the energy through the aperture is measured. A decrease in the transmission through this aperture indicates the onset of limiting and the threshold can be determined by curve fitting to mathematical expressions derived from models of nonlinear interactions. This technique, when applied to materials whose properties have already been published in the technical literature, gave results agreeing with the published results.

The best results were obtained with CBS-100, especially when the fine particles are loosely bound together (the floc state). Threshold fluences as low as 24 mJ/cm^2 for short laser pulses (ns) and 100 mJ/cm^2 for long pulses (μs) have been measured in this suspension. The results indicate also that the bubble generation model for optical limiting in carbon suspensions explain quite well the observed behaviour. An unexpected nonlinear phenomenon appeared in CBS-100 cells (fine state) with a threshold lower than the scattering threshold. That phenomenon could possibly be explained by thermal refraction near laser-heated particles, but this effect is not fully explained yet.

A figure of merit has emerged from these measurements that could be used to order by limiting performance the different types of carbon suspensions. In this ordering, CBS-100 appears as the best choice in the set of suspensions tested for short and long pulses.

The results shown in this document will be used in the comparative studies of different materials exchanged with DERA Malvern (UK) under Annex 16 of the UK/CAN LOA on Co-operation in Defence Science Technology.

Vincent, D.. 2001. Measurement of Optical Limiting Threshold in Various Materials.
TR 2001-028 Defence Research Establishment Valcartier.

UNCLASSIFIED

Sommaire

En raison de l'utilisation de plus en plus fréquente de sources laser telles que les télémètres, les marqueurs et les illuminateurs en général, il faut développer des dispositifs pour protéger les yeux et les capteurs électro-optiques (EO) contre des blessures possibles. Afin de réduire le risque d'endommagement des yeux par un rayonnement laser indéterminé, le CRDV poursuit des recherches sur les matériaux susceptibles d'être utilisés comme limiteurs de rayonnement laser dans les viseurs optiques.

En particulier, de fines particules de carbone en suspension dans un liquide limitent bien le rayonnement visible et proche infrarouge. Afin d'atténuer le rayonnement laser le plus possible tout en maintenant une bonne transmission lumineuse totale, il faut optimiser certains paramètres de la suspension, tels que le choix de la source de carbone, du surfactant et du milieu liquide. Cette optimisation vise à minimiser l'énergie par unité de surface (fluence énergétique) requise pour activer un effet limiteur utile: la fluence de seuil. Une fluence de seuil faible signifie un bas niveau d'énergie limitée et une meilleure protection. Ce rapport fait état des résultats de mesures effectuées sur un ensemble de plusieurs suspensions de carbone différentes, incluant la suspension CBS-100 du CRDV qui, à notre connaissance, offre la meilleure performance contre des impulsions laser courtes et longues et à des taux de répétition jusqu'à 6 ips. Ces mesures ont été prises avec un système optique focalisant simple diaphragmé à $f/20$ et utilisant un petit trou comme fenêtre d'analyse. Le spot laser obtenu en focalisant le faisceau laser dans le matériel non linéaire est réimagé sur le trou d'analyse et l'énergie transmise à travers cette ouverture est mesurée. Une diminution de la transmission à travers cette ouverture indique le début de la limitation optique et le seuil de limitation est déterminé en comparant les mesures à une courbe générée par une relation mathématique issue d'un modèle d'interactions non linéaires. Lorsqu'on l'applique à des matériaux dont les propriétés ont déjà été décrites dans la littérature spécialisée, cette technique donne des résultats conformes à ceux-ci.

Les meilleurs résultats ont été obtenus avec le CBS-100, plus particulièrement lorsque les particules fines étaient mollement reliées ensemble (en "flocons"). Des fluences de seuil de seulement 24 mJ/cm^2 pour les impulsions laser courtes (ns) et 100 mJ/cm^2 pour les impulsions laser longues (μs) ont été mesurées dans cette suspension. Les résultats montrent également que le modèle de génération de bulles comme sources de limitation optique par diffusion non linéaire dans les suspensions de carbone explique bien le comportement observé. Un phénomène non linéaire inattendu a aussi été observé dans le CBS-100 (particules fines) qui présentait un seuil inférieur au seuil de diffusion non linéaire. Ce phénomène encore inexpliqué peut provenir d'une réfraction induite thermiquement près des particules chauffées par laser.

De ces mesures est ressorti un facteur de qualité pouvant servir à classer les différents types de suspension de carbone selon leur pouvoir de limitation. Dans ce classement, le CBS-100 apparaît comme le meilleur choix parmi les suspensions mesurées dans cette étude-ci, que les impulsions soient courtes ou longues.

Les résultats obtenus lors de cette étude serviront aux études comparatives de divers matériaux échangés avec DERA Malvern (RU) dans le cadre de l'annexe 16 de l'entente CAN/RU sur la "Coopération dans les technologies scientifiques de la défense".

Vincent, D.. 2001. Mesure du seuil de limitation optique pour plusieurs matériaux.
TR 2001-028 Centre de recherches pour la défense Valcartier.

UNCLASSIFIED

Table of contents

Abstract.....	i
Résumé.....	i
Executive summary	iii
Sommaire	iv
Table of contents	v
List of figures.....	vi
List of tables	vi
Acknowledgements	vi
Introduction.....	1
Measurement method	2
Results.....	5
Measurements of known materials.....	5
Measurement of DREV CBS-100	7
Discussion.....	11
Conclusion	14
References.....	15
Figures.....	17
Distribution list.....	25

UNCLASSIFIED

List of figures

Figure 1. Measurement system	17
Figure 2. Spot profiles and aperture position in the analysis plane	18
Figure 3. Showing the image A' of the analysis aperture A.....	18
Figure 4. Curve fit for CBS in ethanol.....	19
Figure 5. Curve fit for SiNc in polystyrene.....	19
Figure 6. Curve fit for SiNc in chloroform.....	20
Figure 7. Laser spots in the analysis plane when the focus of L1 is in the cell and out of the cell.....	20
Figure 8. CBS-100 (fine) for short pulses: MMJ fit.....	21
Figure 9. CBS-100 (fine) for short pulses: MMJ and NL fits.....	21
Figure 10. CBS-100 (fine) for short pulses: NL fit.....	22
Figure 11. CBS-100 (flocs) for short pulses: MMJ fit.....	22
Figure 12. CBS-100 (fine) for long pulses: MMJ fit.....	23
Figure 13. CBS-100 (fine) for long pulses: MMJ and NL fits.....	23
Figure 14. CBS-100 (fine) for long pulses: NL fit.....	24
Figure 15. CBS-100 (flocs) for long pulses: MMJ fit.....	24

List of tables

Table 1. Comparison with published values at 532 nm and 13 ns.....	7
Table 2. Values of F_t and α_E/α_0 in various CBS for 13-ns pulses at 532 nm.....	9
Table 3. Values of F_t and α_E/α_0 in various CBS for 1- μ s pulses at 751 nm.....	9
Table 4. Values of $(\alpha_0/\alpha_E)F_{t,MMJ}$ in various CBS for 13-ns and 1- μ s pulses.....	13

UNCLASSIFIED

Acknowledgements

The author wishes to acknowledge the very valuable technical expertise provided by Mr Richard Durand during the course of this project.

UNCLASSIFIED

This page intentionally left blank.

UNCLASSIFIED

Introduction

In the search for materials suitable for optical limiting applications to protect eyes and electro-optical sensors against short-pulse laser radiation, fine carbon particles suspended in a liquid have been shown to possess highly desirable properties: fast switching time (ns), low threshold for nonlinearity, color neutrality and efficient limitation over the visible and near infrared bands while retaining high linear transmission. The three recognized drawbacks of CBS (for "carbon black suspensions") are the less than optimal long-term stability and the reduced nonlinear attenuation for microsecond-long pulses and at high repetition rates. However, by a judicious choice of a carbon powder, a liquid with the appropriate mechanical and thermal properties and a suitable surfactant, DREV's CBS-100 has been shown to limit long pulses quite well and at pulse rates up to 6 pps [1-2]. The long-term stability issue requires further study.

The threshold energy for the onset of optical nonlinearity represents an important parameter while comparing the behaviour of different materials. More precisely, it is the fluence (energy per unit area) at which the attenuating nonlinearity occurs that determines the sensitivity of the materials considered in this work. This publication reports on the measurement of the threshold fluence for optical limiting at nanosecond and microsecond pulses of a high-performance CBS, in an attempt to better understand its behaviour. The validity of the technique has been tested by measurements on materials whose properties can be found in the technical literature. This work has been carried out at DREV from January to October 2000 under Work Unit 2km21, "Eye and Sensor Protection against Laser Radiation".

UNCLASSIFIED

Measurement method

In order to measure the peak (on-axis) fluence in a limiter cell, the optical arrangement shown in Fig. 1 has been used. The laser sources were either a doubled-Nd:YAG laser emitting 13-ns pulses at 532 nm or a modified alexandrite laser emitting 1- μ s pulses at 751 nm [3]. After appropriate attenuation by an arrangement of glass attenuators and halfwaveplate/polarizer attenuators and a 10 \times expansion, the laser beam is apertured to $f/20$ at lens L1 which focusses it inside the test cell. Lens L2 recollimates the beam and lens L3 focusses it again on the analysis plane containing aperture A. In fact, the lens arrangement L2-L3 images the laser spot in the cell onto the analysis plane with a lateral magnification of 25 \times . The analysis aperture A has a diameter d_A smaller than the FWHM of the unaffected low-energy spot, as shown in Fig. 2. This analysis aperture can be considered as defining a measurement aperture A' at the spot position (in the cell) of area $(\pi d_A^2/4)/25^2$, as shown in Fig. 3. By adjusting precisely the focal plane of L1 in the center of the cell and the image of the focal spot on A, then the average fluence at A' is given by

$$F_{\text{int}} = T_A \sqrt{T_0} E_{\text{in,ext}} / ((\pi d_A^2/4)/25^2) \quad (1)$$

where

T_A is the transmission of the aperture (its overlap integral with the spot profile)

T_0 is the external cell's transmission, and

$E_{\text{in,ext}}$ is the input pulse energy measured outside the cell.

Experimentally, d_A equals 0.2 mm (so $d_{A'} = 8 \mu\text{m}$), and $T_A T_0$ is the total linear transmission through the cell and through A, such that (1) becomes

$$F_{\text{int}} = 1.99 \times 10^6 T_A T_0 E_{\text{in,ext}} / \sqrt{T_0} \quad (\text{J/cm}^2). \quad (2)$$

At $f/20$, the FWHM for a diffraction-limited spot is 20λ (within 3 %), which corresponds to 10.6 μm at $\lambda=532$ nm, and to 15.0 μm for $\lambda=751$ nm. The experimental values obtained were respectively $11.7 \pm 0.3 \mu\text{m}$ and $15.9 \pm 0.3 \mu\text{m}$. Thus, the spot was almost diffraction-limited in

UNCLASSIFIED

both cases. Accordingly, the depth-of-focus, given approximately by $4.88 \times 10^2 \times \lambda$ equals 1.04 mm at 532 nm, and 1.47 mm at 751 nm. These values are comparable to the cell's liquid pathlength of 2mm and, near threshold, the laser beam can be considered as collimated in the nonlinear region. These values of spot's FWHM are significantly larger than 8 μm , the value of d_A .

By measuring the usual transfer function $E_{out, ext}$ through the aperture A with respect to $E_{in, ext}$ and by fitting functions to the experimental data, it is possible to determine the threshold fluences for the different phenomena involved. These threshold values depend on the models from which the fitting functions are derived. Experimentally, two different functions were found to fit the data well enough as to lead to meaningful threshold values. The first one represents the solution to the nonlinear Beers-Lambert equation expressed in terms of fluence [4]

$$dF/dz = -\alpha F - \beta F^2 \quad (3)$$

where α gives the low-energy linear attenuation (mainly absorption), and β , the high-energy nonlinear attenuation (not necessarily absorption). Integration along the cell pathlength for a collimated beam (and taking into account the transmission at the input and output surfaces T_s) leads to

$$F_{out} = T_0 F_{in} / (1 + T_s F_{in} / F_{sat}) \quad (4)$$

where F_{in} and F_{out} are the input and output fluences outside the cell, $T_0 = T_s^2 e^{-\alpha L}$ and $F_{sat} = \alpha / \beta (1 - T_0 / T_s)$. Using $T_s F_{in} / F_{sat} = E_{in} / E_{sat}$ (from (2)) and $T_{NL} = E_{out} / T_0 T_A E_{in} = F_{out} / T_0 F_{in}$ where E_{out} is measured through the analysis aperture, then the nonlinear transmission is

$$T_{NL} = 1 / (1 + E_{in} / E_{sat}) \quad (5)$$

Defining $E_t = \gamma E_{sat}$, then, at $E_{in} = E_t$, $T_{NL} = 0.5$ if $\gamma = 1$ and $T_{NL} = 0.909$ if $\gamma = 0.1$. In the following, the threshold energy E_t for this fit is defined at $\gamma = 0.1$, which means that $E_{out} / E_{in} = 0.909 T_0 T_A$. Different definitions of E_t can be compared by the relation

$$E_{t1} = ((1 - T_{NL,1}) / T_{NL,1}) (T_{NL,2} / (1 - T_{NL,2})) E_{t2} \quad (6)$$

UNCLASSIFIED

Using the definition for T_{NL} and (5), the fitting equation containing measurable quantities reads as

$$E_{out} = T_0 T_A E_{in} / (1 + 0.1 E_{in} / E_t) \quad (7)$$

where E_t is the only adjustable parameter. This will be referred to as the NL fit in this paper.

The second fitting function comes from the "bubble wavefront" model proposed by McEwan, Milsom and James [5]. In this model, the transmission of a collimated beam (a plane wave) through the cell is linear until the input energy is high enough to initiate a thin layer of bubbles with a different attenuating coefficient. Increasing further the energy creates a second layer of bubbles after the first one, and so on until the volume of the cell is filled with bubbles. In the geometry considered here, the first layer of bubbles would form at the focal plane and the subsequent layers would form towards the input window. Apart from that, the situation is quite similar near threshold. The relation given in [5] expresses the transmission in the bubble regime as

$$T = T_0 (E_t / E_{in}) (1 + (\alpha_e / \alpha_0) ((E_{in} / E_t) - 1))^{\alpha_0 / \alpha_e} \quad (8)$$

where α_0 is the linear absorption coefficient and α_e , the nonlinear extinction coefficient. Using $E_{out} = T_A \times \text{total output energy}$ and $m = \alpha_0 / \alpha_e \leq 1$, (8) becomes in terms of measurable quantities

$$E_{out} = T_0 T_A E_t (1 + m^{-1} ((E_{in} / E_t) - 1))^m \quad (9)$$

where E_{out} is measured through the aperture A , m is the slope of a log-log plot of E_{out} against E_{in} for $E_{in} / E_t \gg 1$ and E_t is the only adjustable parameter. Equation 9 will be referred to as the MMJ fit (for McEwan-Milsom-James) in this paper.

Before proceeding to the presentation of the results, it seems appropriate to discuss briefly the effect of aperture $A2$ in Fig. 1. When $L1$ is apertured to $f/20$ by $A1$, the sensitivity for threshold determination, especially in the case of a scattering cell, should increase by aperturing also $L2$ to $f/20$ using $A2$. However, it has been found experimentally that the sensitivity increase, albeit present, was not large enough to justify the use of $A2$. Since the adjustments of the cell's position and of the optical system are made at $f/5$ before aperturing to $f/20$, it was decided to leave $A2$ at $f/5$ and even at a larger aperture.

UNCLASSIFIED

Results

Measurement of known materials

Before undertaking the measurement of DREV CBS-100, it seemed worthwhile to get confidence in this technique by measuring various materials whose limiting thresholds have already been published. These measurements were taken with 13-ns pulses at 532 nm where most of the data appear. Figures 4, 5 and 6 show the results of measurements on three well-known materials: carbon black suspension in ethanol, SiNc (in the form $\text{SiNc}[\text{OSi}(\text{n-C}_6\text{H}_{13})_3]_2$ as in Ref. 6) in polystyrene and SiNc in chloroform. The dashed straight lines in Fig. 4 allow the evaluation of $T_A T_0$ and m , and (9) is used to find E_t by iteration and to draw the MMJ fit. Note that (9) is valid only for $E_m > E_t$. For $E_m < E_t$, the suspension behaves linearly in this model. Fig. 5 displays typical nonlinear absorption data. $T_A T_0$ was found as in Fig. 4 and (7) was used to determine E_t by fitting the calculated curve to the data. Finally, Fig. 6 shows what happens when SiNc is measured in a liquid (chloroform). The low-energy portion of the data agrees well with (7), as represented by the dot curve, but the full line given by (9) fits better the high-energy portion. That means that scattering from bubbles arises at $E_m > 65$ nJ. Note that the low-energy $T_A T_0$ is used in (7), and the value of $T_A T_0$ at threshold for scattering is used in (9). The two curves fit the data for the values of E_t and m listed in Fig. 6. It was not possible to fit all the data with the NL fit only. This situation arose even in some CBS limiters as will be shown later.

Table 1 compares the measured values of F_t to some values found in the literature. In the measured suspensions, the carbon particle diameter ranged from 30 to 200 nm with most of the diameters between 70 and 100 nm. For CBS in CHCl_3 and in ethanol, the agreement is good but the published values in water and a mixture of water and ethylene glycol (EG) are about twice our measured values. Mansour et al. [9] used a 50:50 mixture of water-EG, whereas the mixture used in the present work was 66% of water by volume. Perhaps the greater viscosity of EG impedes the development of bubbles, thus increasing the value of input energy for an observable change in transmission. However, it seems more likely that the presence of residual surfactant agents from the initial ink component could change the high surface tension of the liquid mixture containing water to such an extent that appreciable changes in F_t would occur. This depends a lot on the composition of the ink. Of prime

UNCLASSIFIED

importance for what follows is the fact that the trend in F_T values from CHCl_3 to water is the same in both sets of values and that the agreement is good at low threshold values. For nonlinear absorbing materials such as RSA dyes, it is more difficult to compare the values obtained using the analysis aperture technique with the published values because the change is more gradual than the sudden change occurring in CBS (in the bubble model) and a criterion must be defined for the threshold (as $\gamma = 0.1$ in (7)). In the papers collected for the comparison, the authors used a quasi-collimated beam and measured the total output energy (except possibly in Ref. 12, where a diffuser is used in front of the detector). A 9% decrease in output energy through the analysis aperture in Fig. 2 corresponds approximately to a 2 to 3% decrease in total output energy since, at threshold, only the peak changes and the aperture collects about 25% of the total output energy (as shown in Fig. 7). Accordingly, the interpolated values from published graphs at $T = 0.97T_0$ have been incorporated in Table 1. The published value for SiNc/toluene agrees quite well with the measured value in chloroform. The agreement is good also for C_{60} in toluene, except with Ref. 12, but the irradiation geometry (rod's end imaged on the cell) and the detection arrangement (diffuser in front of detector) are different in this case. Finally, the published value for CAP/ethanol differs slightly from our measured value but the interpolation cannot be made so accurately with the graph published in Ref. 13. CAP (Aluminum Phthalocyanine Chloride) was obtained initially from Kodak but can now be bought from Aldrich, and C_{60} came from SES Research Inc. (Houston, Texas, USA) and Pyrogenesis (Montréal, Québec, Canada).

From this comparison it is believed that the analysis aperture technique allows the accurate measurement and ordering of thresholds in optical limiting materials.

UNCLASSIFIED

Table 1. Comparison with published values at 532 nm and 13 ns

NONLINEAR MATERIAL	F_t (J/cm ²)	F_t (J/cm ²)
CBS	Measured	Published
• ink in chloroform	0.04	0.034 (Refs. 5, 7)
• ink in ethanol	0.07	0.06 (Ref. 8) (a)
• ink in water	0.09	0.17 (Ref. 7)
• ink in water+ethylene glycol	0.08	0.20 (Ref. 9)
Others	$\gamma = 0.1$	$T = 0.97 T_0$
• C ₆₀ in toluene	0.017	0.013 (Ref. 10)
		0.02 (Ref. 11)
		0.05 (Ref. 12)
in chlorobenzene	0.046	
in PMMA	0.01	
• CAP in ethanol	0.008	0.006 (Ref. 13)
• SiNc in chloroform	0.004	
in polystyrene	0.008	
in PMMA	0.013	
in toluene		0.004 (Ref. 4) (b)

(a) $E_t = 1 \mu\text{J}$, $\text{FW1}/e^2M = 65 \mu\text{m}$, focus in the center of the cell, $T_0 = 0.81$ and assuming that the spot has a near-Gaussian shape.

(b) $E_t = 5 \text{ nJ}$, $\text{HW1}/e^2M = 8 \mu\text{m}$, focus in the center of the cell, $T_0 = 0.59$ and assuming $F^* > 15$.

Measurement of DREV CBS-100

The proprietary recipe of DREV's carbon suspension CBS-100 starts from a mixture of carbon powder and surfactant disrupted ultrasonically at high power. The resulting paste was dispersed into an organic solvent with the appropriate surfactant, passed through a filter with 100 nm pores and diluted to the required concentration. The prepared material was also kept sealed in darkness. For optical limiting measurements, custom-made cells were used to

UNCLASSIFIED

contain the limiting materials. The liquid pathlength can be varied between 1 and 4 mm, but the results presented below come mostly from cells with a 2-mm pathlength and some results with dyes come from cells with a 1.5-mm pathlength. The ordinary glass windows have a refractive index near 1.5. All the cells were sealed under vacuum with a vapour space left in them to absorb the laser-induced shock waves and to ease the formation of laser-induced bubbles. CBS-100 appears in two different states, depending on the ageing status (Refs. 1-2). Fresh suspensions, or ultrasonically shaken ones, contain very fine carbon particles (approximately $10^{13}/\text{cm}^3$ [14]) with an equivalent diameter less than 60 nm as measured with a laser particle sizer, whereas cells aged for a few weeks contain larger loosely bound carbon particles called flocs (see "The Concise Oxford Dictionary" 1990 p.451). These flocs are easily reconverted to fine particles by ultrasonic shaking. The limiting performance results given below are usually different for the two states.

Results with 13-ns pulses at 532 nm

The input-output characteristic at $f/20$ was measured with many cells of different T_0 in the fine and the floc states. In Figs. 8-10 are plotted three representative results obtained with different cells containing the suspension in the fine state. In Fig. 8, the MMJ model fits quite well the data points. In Fig. 9, both NL model and MMJ model are required to fit the data points. Finally, in Fig. 10, even if it is a true scatterer at high input energy, this suspension behaves like a continuous NL attenuator near threshold (observed in one cell only). However, in the floc state, the MMJ model fitted all the data points very well and one example appears in Fig. 11. Thus, two nonlinear mechanisms seem to occur in CBS-100 while in the fine state: one explosive mechanism explainable by the generation of bubbles and another one related possibly to the heating of the liquid near a very small carbon particle causing a continuous change in refraction or scattering leading to an increase in attenuation. Since this last mechanism was not observed with nanosecond pulses in ink-based suspensions prepared in the same host liquid with the same surfactant or in other liquids, it is suggested that the combination of the smaller carbon particles in CBS-100 (fine) and the host fluid used allows this mechanism to be strong enough in some cells to be observed. However, above the threshold for the bubble regime, scattering from bubbles predominates. The continuously attenuating mechanism is observed also with microsecond pulses in some fine particle suspension where the bubble threshold is higher, as will be shown later. The fact that this mechanism is not observed in floc state indicates the importance of small particles to obtain it. Table 2 lists the values of $F_{i,NL}$, $F_{i,MMJ}$ and α_E/α_0 for the suspensions studied.

UNCLASSIFIED

Table 2. Values of F_t and α_E/α_0 in various CBS for 13-ns pulses at 532 nm

NONLINEAR MATERIAL	α_E / α_0	$F_{t,NL}$ (J/cm ²)	$F_{t,MMJ}$ (J/cm ²)
• CBS-100 (flocs)	4	---	0.024
• CBS-100 (fine)	6	0.02	0.04
• ink in chloroform with surfactant (fine)	3.5	---	0.04
• ink in chloroform w/o surfactant (fine)	5	---	0.06
• ink in ethanol w/o surfactant (fine)	5.5	---	0.07
• ink in water (fine)	3	---	0.09
• ink in water+ethylene glycol (fine)	4	---	0.08

Results with 1- μ s pulses at 751 nm

The graphs in Fig. 12-14 show some examples of results obtained with 1- μ s pulses at 751 nm. They correspond to a MMJ fit in Fig. 12, a NL and a MMJ fit in Fig. 13 and a NL fit in Fig. 14 (same cell as in Fig. 10). Only the MMJ model could fit the data points in the floc state for all the cells. An example of data obtained in the floc state appears in Fig. 15. The continuously attenuating mechanism was observed in CBS-100 (fine) and in an ink-based suspension in chloroform with and without surfactant. The higher threshold for bubble

Table 3. Values of F_t and α_E/α_0 in various CBS for 1- μ s pulses at 751 nm

NONLINEAR MATERIAL	α_E / α_0	$F_{t,NL}$ (J/cm ²)	$F_{t,MMJ}$ (J/cm ²)
• CBS-100 (flocs)	2×10^1	---	0.1
• CBS-100 (fine)	6	0.06	0.16
• ink in chloroform with surfactant (fine)	6	0.13	0.2
• ink in chloroform w/o surfactant (fine)	4	0.15	0.2
• ink in ethanol w/o surfactant (fine)	5	---	0.5
• ink in water (fine)	2×10^1	---	2×10^1
• ink in water+ethylene glycol (fine)	1×10^1	---	2×10^1

UNCLASSIFIED

formation with microsecond long pulses facilitates the observation of this mechanism in suspensions containing slightly larger particles. Table 3 lists the values of $F_{i,NL}$, $F_{i,MMJ}$ and α_E/α_0 for the suspensions studied.

UNCLASSIFIED

Discussion

From the results presented in the previous sections, it appears clearly that the performance of carbon suspensions, at an input fluence where scattering predominates, is well represented by a relation derived from a model based on the explosive generation of bubbles. At lower fluences, the transmission is either linear or slightly nonlinear. Possibly, this nonlinearity comes from the heating of the highly thermally sensitive liquid surrounding very small particles. For 13-ns pulses, it occurred only in the suspensions having the smallest particles, whereas suspensions having somewhat larger particles exhibit a similar behaviour against 1- μ s pulses. However, this effect seems to exist only with very small particles since it has not been observed with flocs.

The data in Tables 2 and 3 indicate that the lowest $F_{t,MMJ}$ occurs in CBS-100 (flocs) with both nanosecond and microsecond pulses. However, α_E / α_0 is lower with CBS-100 (flocs) than with CBS-100 (fine) for 13-ns pulses, meaning that the nonlinear attenuation is smaller in flocs near threshold with short pulses since the values of α_0 in the floc and the fine state differ by less than 7%. The situation is quite different with microsecond pulses, where α_E / α_0 is about four times larger in CBS-100 (flocs) than in any other mixture (excluding water) while its $F_{t,MMJ}$ is the lowest one. Due to the high threshold value in water mixtures, the heating is so strong that the bubble size increases rapidly enough during the 1- μ s pulse to lead to a high value of α_E / α_0 . However, the increase is not fast enough for 13-ns pulses, thus the low value of α_E / α_0 in mixtures containing water. These values for water listed in Table 2 agree quite well with the values (3.3 and 3.9) given in Ref. 5 for a mixture of water-methanol in the proportion 4:1.

An interesting parameter coming out of the values listed in Tables 2 and 3 and allowing some sorting of the various materials can be written as $(\alpha_0 / \alpha_E) F_{t,MMJ}$. Table 4 gives its value for the various suspensions studied. A low value of this parameter indicates a material with good optical limiting performance as can be seen from (9) for $E_{in} / E_t \gg 1$. With 13-ns pulses, its value decreases from water-based suspensions to more volatile organic solvents, and by changing to a different starting carbon material. Its values for CBS-100 in the fine and floc state are practically the same and lower than the values for ink in organic solvents, these two

UNCLASSIFIED

results being consistent with the results of optical limiting in an $f/5$ system published in Refs. 2 and 15. With 1- μ s pulses, its value decreases from water to ethanol (due mainly to a lower surface tension in ethanol), then from ethanol to chloroform (due to a lower heat capacity, a lower volumic heat of vaporization and a lower thermal conductivity in chloroform), and from chloroform to chloroform with surfactant (due to a lower surface tension with surfactant). Its value decreases again from ink-based suspensions to CBS-100 (fine) and there is a large decrease from CBS-100 (fine) to CBS-100 (flocs) due possibly to the coalescence of many small bubbles into one large bubble in a floc. These results are also consistent with those obtained with an $f/5$ system presented in Refs. 2 and 15.

The values listed in Tables 1-4 do not reflect the precision of each measurement but rather the sample-to-sample variations for the same material. The determination of E_t , T_0 , and T_0T_A is precise to within 1-3% each and the determination of α_0/α_E is precise within 2-10% depending on the cell, such that the precision is about 3-7% on F_t and 5-17% on $(\alpha_0/\alpha_E)F_t$. However, cell-to-cell variations can amount to a factor of 2. Thus the values in Tables 1-4 represent rounded-off values of ensemble averages over cells of various T_0 for CBS-100 and ink-chloroform. The same number-rounding has been applied to the other materials for which only one or two cells have been measured. The values in Table 4 have been calculated before the round-off given in Tables 2 and 3, so some differences can occur in checking values in Table 4 from the values in Tables 2 and 3. Finally, a 30-50% change in Table 4 represents a very significant change in behaviour.

UNCLASSIFIED

Table 4. Values of $(\alpha_0/\alpha_E)F_{t,MMJ}$ in various CBS for 13-ns and 1- μ s pulses

NONLINEAR MATERIAL	$(\alpha_0/\alpha_E)F_{t,MMJ}$ (J/cm ²)	
	13 ns	1 μ s
• CBS-100 (flocs)	0.006	0.005
• CBS-100 (fine)	0.007	0.03
• ink in chloroform with surfactant (fine)	0.01	0.035
• ink in chloroform w/o surfactant (fine)	0.01	0.06
• ink in ethanol w/o surfactant (fine)	0.01	0.09
• ink in water (fine)	0.03	1
• ink in water+ethylene glycol (fine)	0.02	2

UNCLASSIFIED

Conclusion

The series of measurements reported here indicate that a mathematical relation derived from a model based on the formation of bubbles in CBS represents quite well the nonlinear transmission of CBS near the threshold for optical limiting. Albeit not being a formal proof, it is a clear indication of the applicability of this model. Another conclusion drawn from these results is that the parameter $(\alpha_0 / \alpha_E) F_{i,MMJ}$ allows an ordering of the efficiency of different types of suspensions: the lower the parameter, the higher is the efficiency. From all the suspensions reported in this publication, DREV CBS-100 (floc state) has the lowest value of this parameter and offers the best performance against short pulses (ns) and long pulses (μ s). Finally, the analysis-aperture technique as described here appears as a suitable tool for measuring optical limiting threshold with low-energy laser pulses. The same testbed used to measure the threshold at $f/20$ (in a 0.2-mrad aperture A) can also measure the optical limiting performance for eye protection at $f/5$ (in a 1.5-mrad aperture A) simply by adjusting apertures A1 and A. This analysis-aperture technique applies equally well to nonlinear absorbers and nonlinear absorbers with a scattering component, as shown by the results obtained with dyes and C₆₀ in plastics and in liquids.

UNCLASSIFIED

References

1. Vincent, D., "High-Performance Optical Limiter Based on Fine Carbon Particles Suspended in an Organic Solvent", *Nonlinear Optics*, Vol. 21, pp. 413-422, 1999.
2. Vincent, D., "Optical Limiting with Carbon Suspensions at Selected Wavelengths and Pulse Lengths", *Jour. of Nonlinear Optical Physics and Materials*, Vol. 9, No. 3, pp. 243-259, 2000.
3. Vincent, D. and Mathieu, P., "Trois modes d'opération d'un laser à tige d'alexandrite: impulsions laser de 0.1, 1 et 100 μ s", DREV TN-1999-133, octobre 1999, SANS CLASSIFICATION.
4. Hagan, D.J., Xia, T., Said, A.A. and Van Stryland, E.W., "Tandem Limiter Optimization", *SPIE Proc.* Vol. 2229, pp. 179-190, 1994.
5. McEwan, K.J., Milsom, P.K. and James, D.B., "Nonlinear Optical Effects in Carbon Suspensions", *SPIE Proc.* Vol. 3472, pp. 42-52, 1998.
6. Wheeler, B.L., Nagasubramanian, G., Bard, A.J., Schechtman, L.A., Dininny, D.R. and Kenney, M.E., "A Silicon Phthalocyanine and a Silicon Naphthalocyanine: Synthesis, Electrochemistry, and Electrogenerated Chemiluminescence", *Jour. Am. Chem. Soc.* Vol. 106, pp. 7404-7410, 1984.
7. James, D.B. and McEwan, K.J., "Bubble and Refractive Processes in Carbon Suspensions", *Nonlinear Optics*, Vol. 21, pp. 377-389, 1999.
8. Nashold, K.M. and Powell Walter, D., "Investigations of Optical Limiting Mechanisms in Carbon Particle Suspensions and Fullerene Solutions", *Jour. Opt. Soc. Am. B*, Vol. 12, pp.1228-1237, 1995.
9. Mansour, K., Soileau, M.J. and Van Stryland, E.W., "Nonlinear Optical Properties of Carbon-Black Suspensions (ink)", *Jour. Opt. Soc. Am. B*, Vol. 9, pp. 1100-1109, 1992.
10. Li, C., Zhang, L., Wang, R., Song, Y. and Wang, Y., "Dynamics of Reverse Saturable Absorption and All-Optical Switching in C_{60} ", *Jour. Opt. Soc. Am. B*, Vol. 11, pp. 1356-1360, 1994.
11. McLean, D.G., Sutherland, R.L., Brant, M.C., Brandelik, D.M., Fleitz, P.A. and Pottenger, T., "Nonlinear Absorption Study of a C_{60} -toluene Solution", *Opt. Lett.* Vol. 18, pp. 858-860, 1993.
12. Tutt, L.W. and Kost, A., "Optical Limiting Performance of C_{60} and C_{70} solutions", *Nature* Vol. 356, pp. 225-226, 1992.
13. Brunel, M., Canva, M., Brun, A., Chaput, F., Malier, L. and Boilot, J.-P., "Doped Gels for Optical Limiting Applications", *Mat. Res. Soc. Symp. Proc.* Vol. 374, pp. 281-286, 1995.

UNCLASSIFIED

14. Calculated by Dr Luc Bissonnette at DREV from the particle distribution measured with a laser particle sizer.
15. Vincent, D. and Durand, R., "Optical Limiting with Carbon Suspensions at Different Wavelengths and Pulse Lengths (U)", DREV TR 1999-152, March 2000, CONFIDENTIAL.

UNCLASSIFIED

Figures

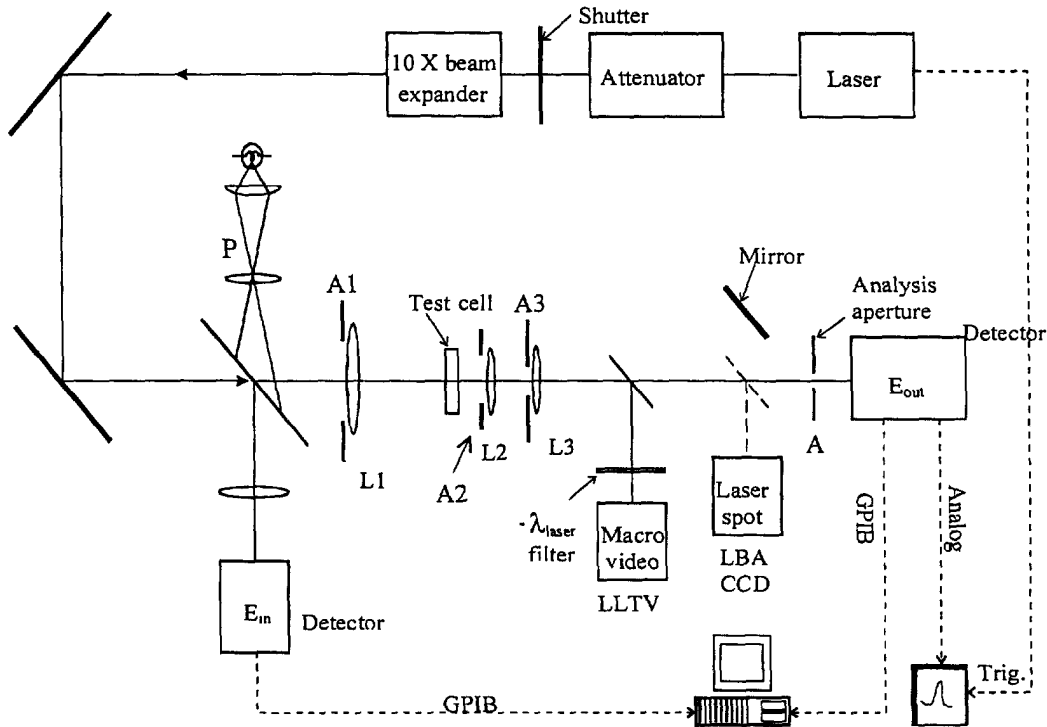


Figure 1. Measurement system LLTV is a low level TV which allows the observation of particles' movement in the cell illuminated by the projector P, but the light is off during the nonlinear transmission measurements LBA is a laser beam analyzer with a CCD camera which allows the observation of the laser spot when the angled mirror is in position. The output pulse can be seen on an oscilloscope and the data are collected by a dedicated computer.

UNCLASSIFIED

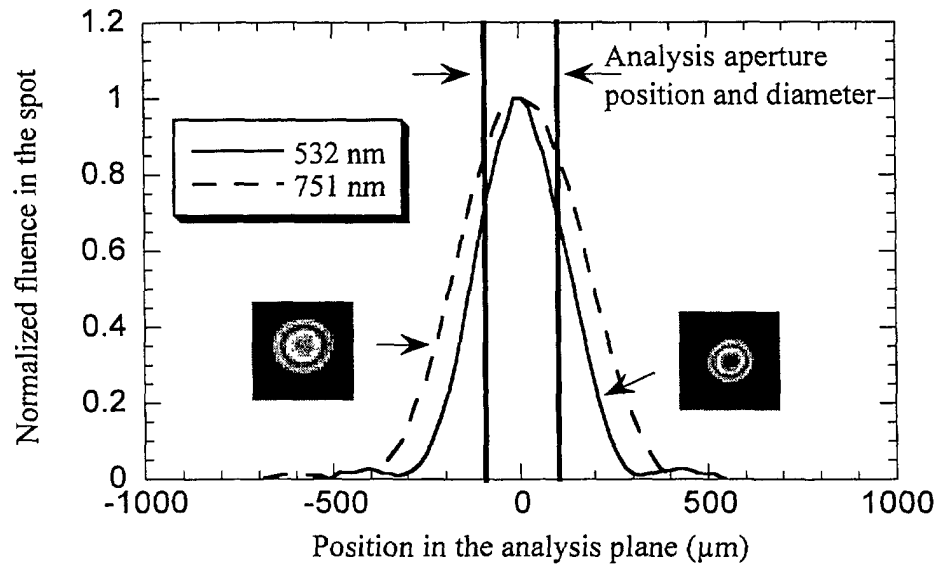


Figure 2. Spot profiles and aperture position in the analysis plane, the photographs show that the constant fluence contours in the spot are circular.

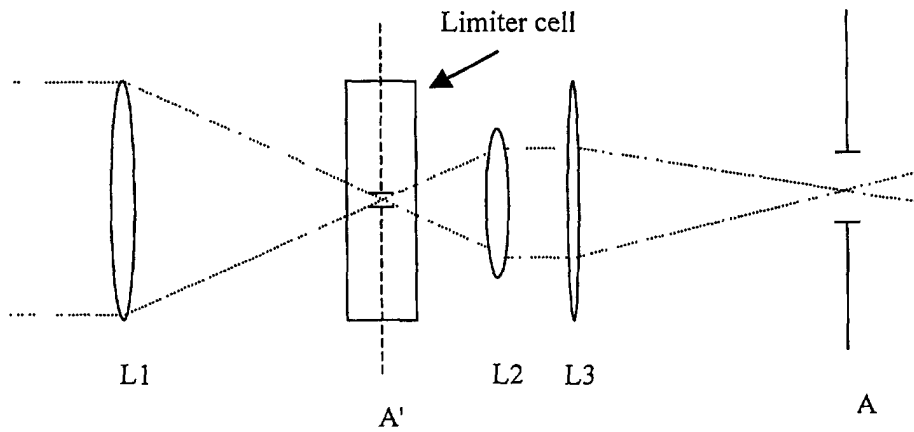


Figure 3 Showing the image A' of the analysis aperture A

UNCLASSIFIED

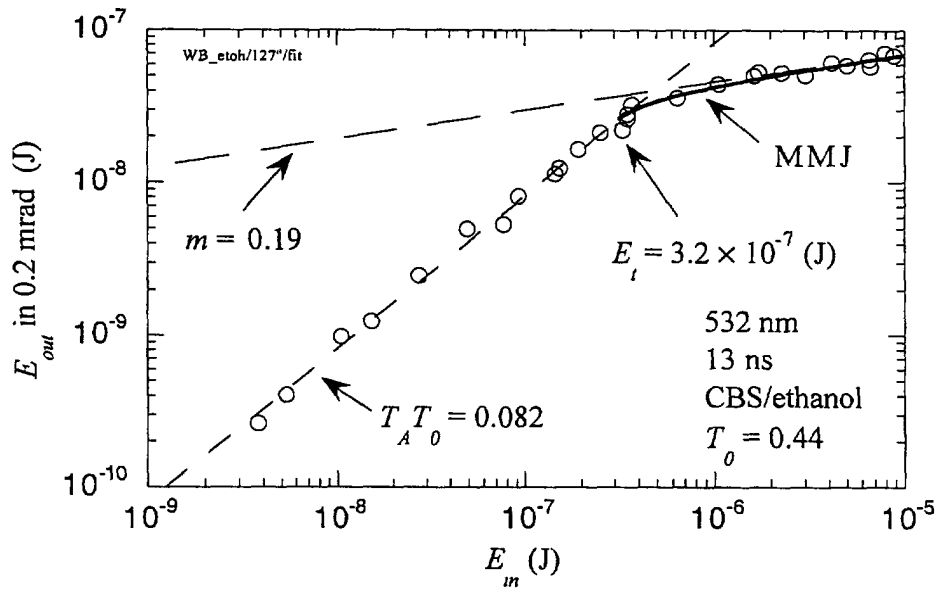


Figure 4. Curve fit for CBS in ethanol

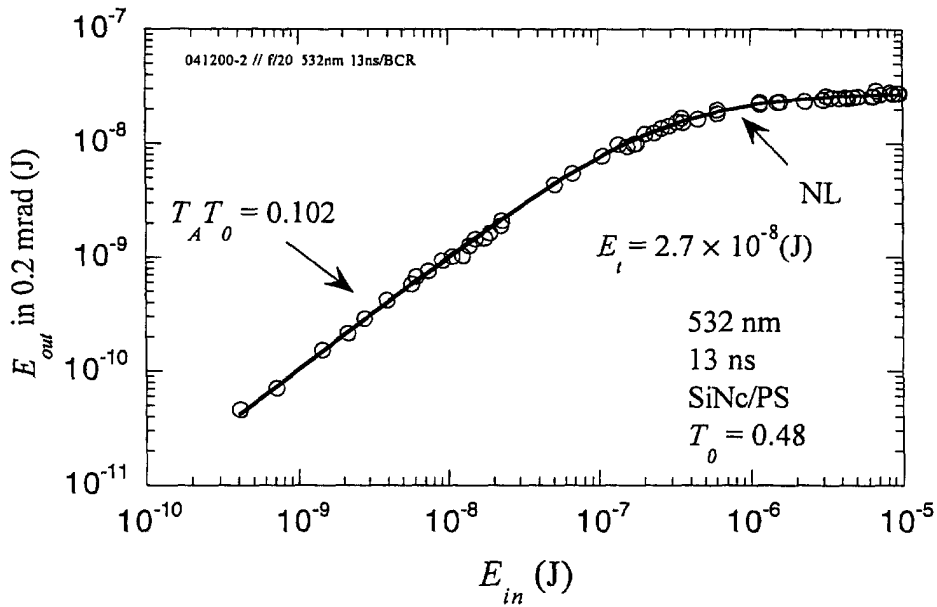


Figure 5. Curve fit for SiNc in polystyrene

UNCLASSIFIED

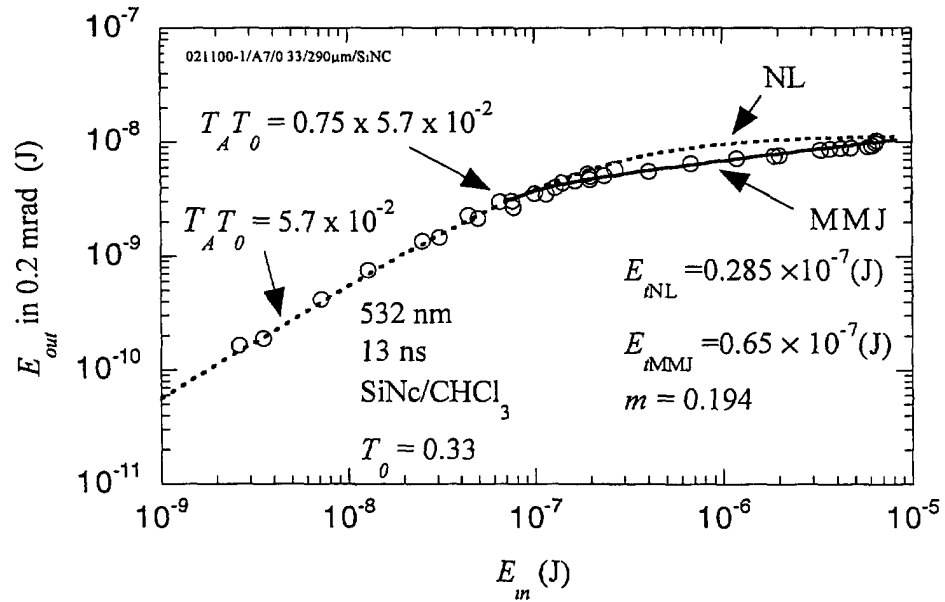


Figure 6. Curve fit for SiNc in chloroform

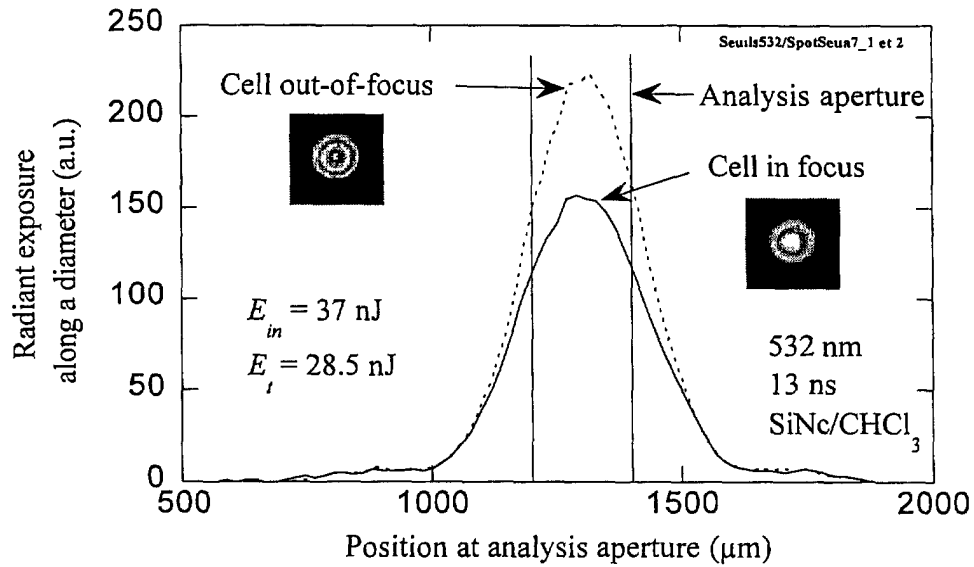


Figure 7. Laser spots in the analysis plane when the focus of L1 is in the cell and out of the cell. The figure shows that the change in measured energy is much larger through the aperture than in the full spot.

UNCLASSIFIED

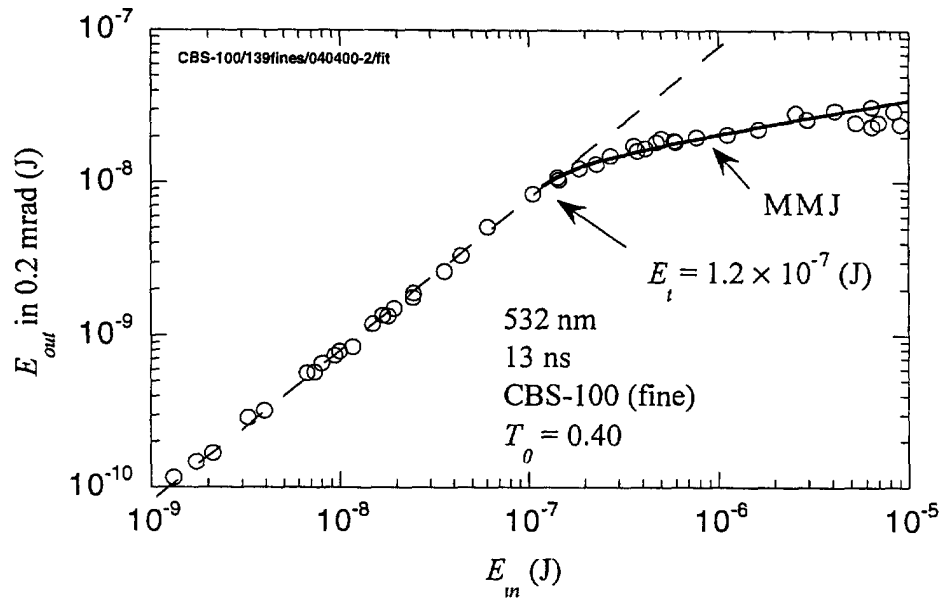


Figure 8. Threshold determination in a sample of CBS-100 (fine) for short pulses: MMJ fit

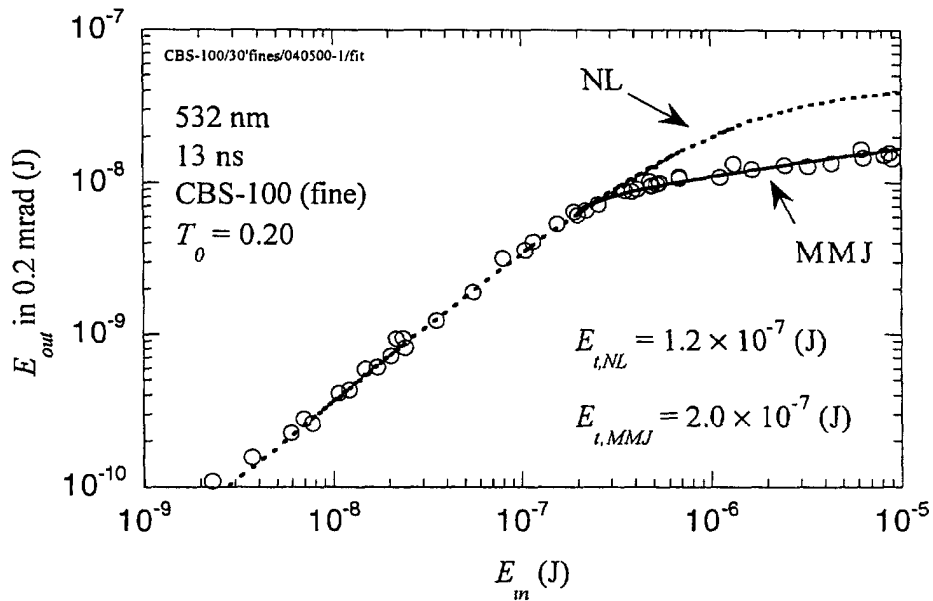


Figure 9. Threshold determination in a sample of CBS-100 (fine) for short pulses: MMJ and NL fits

UNCLASSIFIED

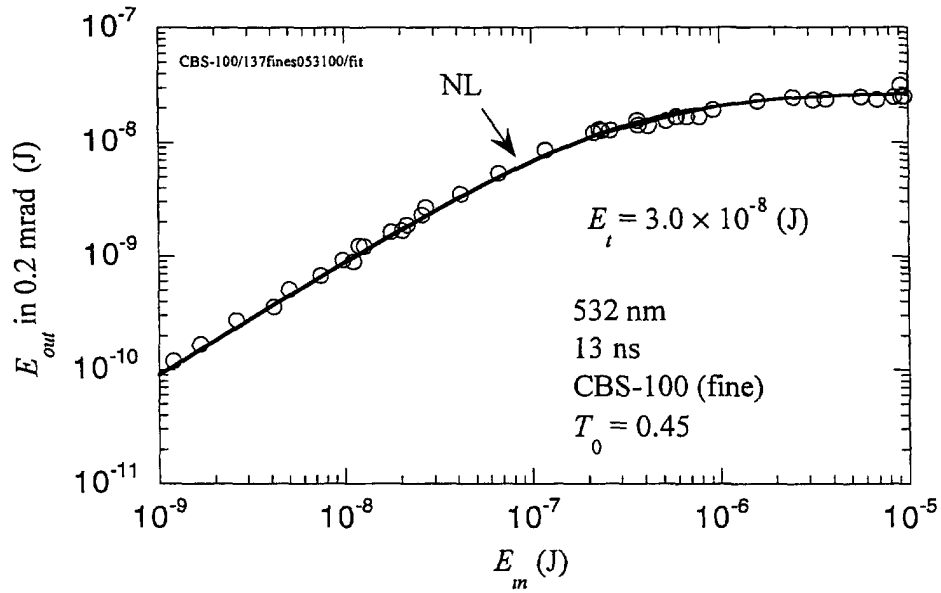


Figure 10. Threshold determination in a sample of CBS-100 (fine) for short pulses: NL fit

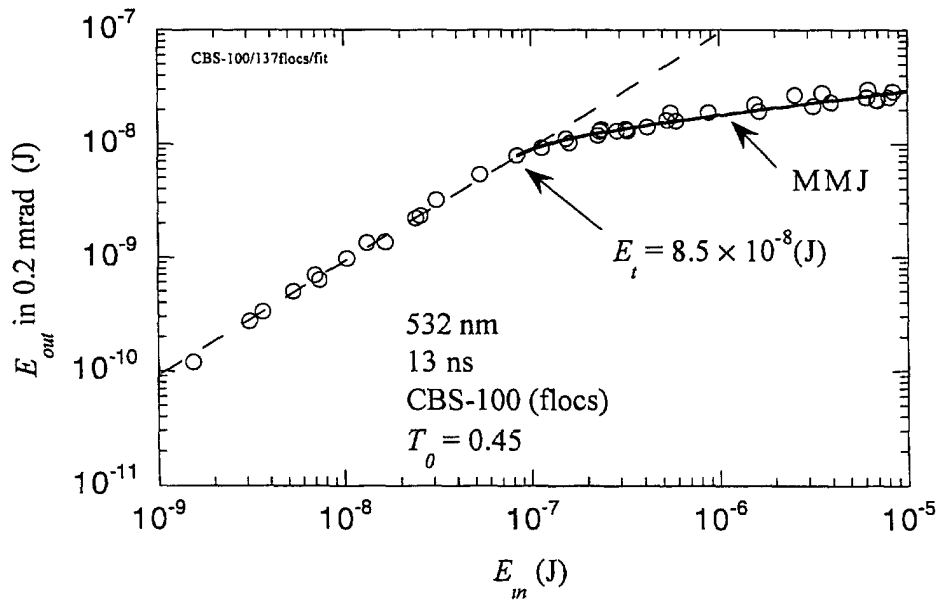


Figure 11. Threshold determination in a sample of CBS-100 (flocs) for short pulses. MMJ fit

UNCLASSIFIED

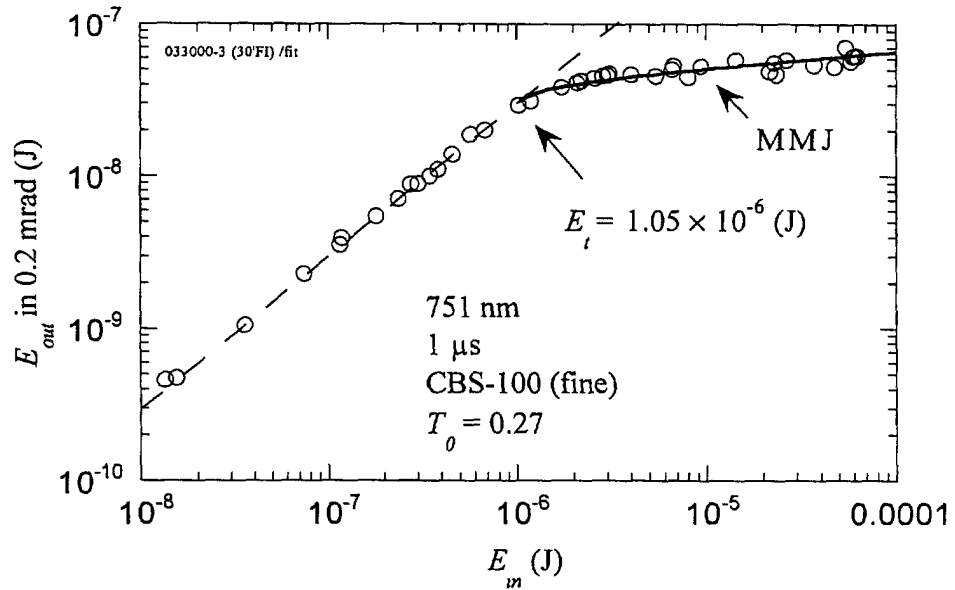


Figure 12. Threshold determination in a sample of CBS-100 (fine) for long pulses. MMJ fit

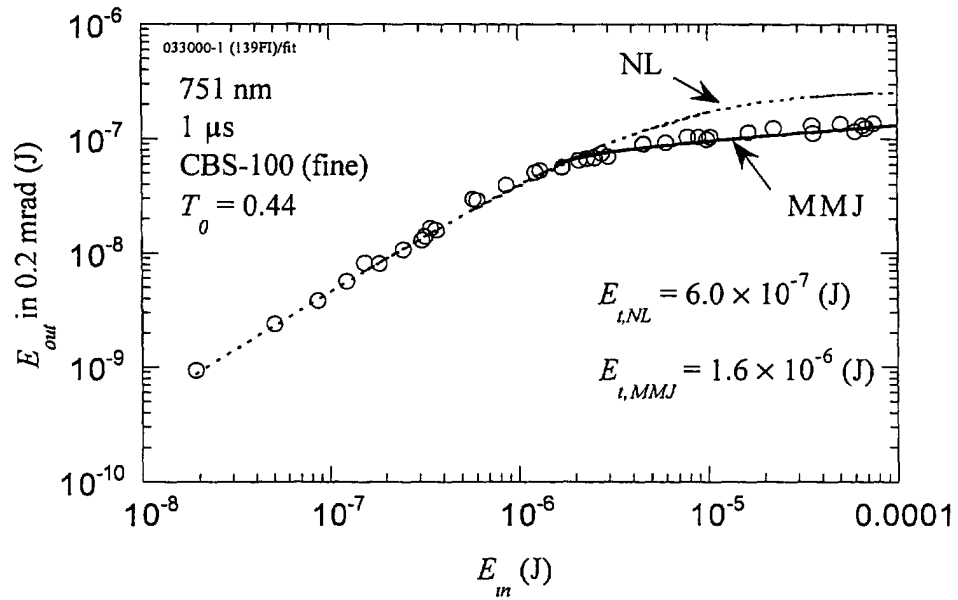


Figure 13. Threshold determination in a sample of CBS-100 (fine) for long pulses. MMJ and NL fits

UNCLASSIFIED

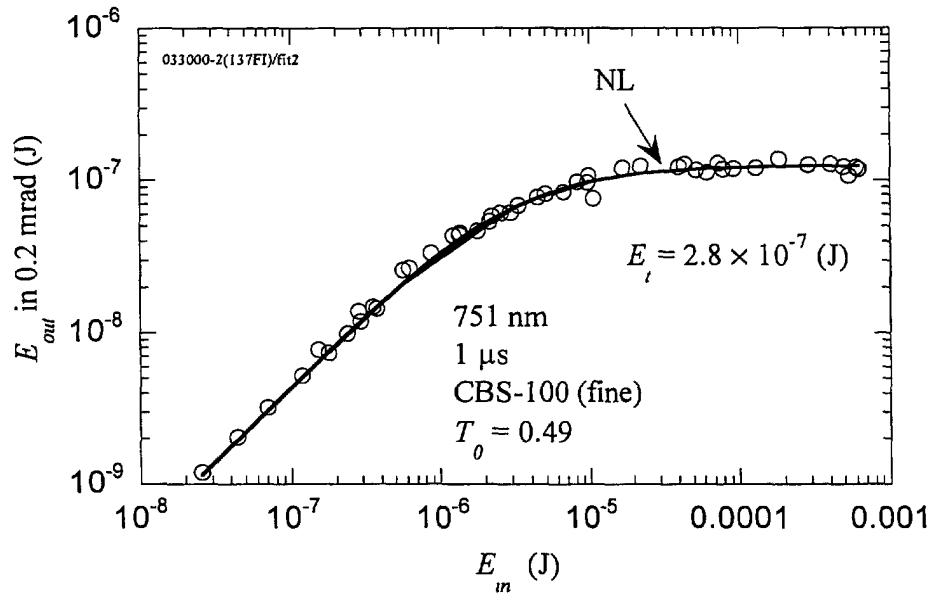


Figure 14. Threshold determination in a sample of CBS-100 (fine) for long pulses: NL fit

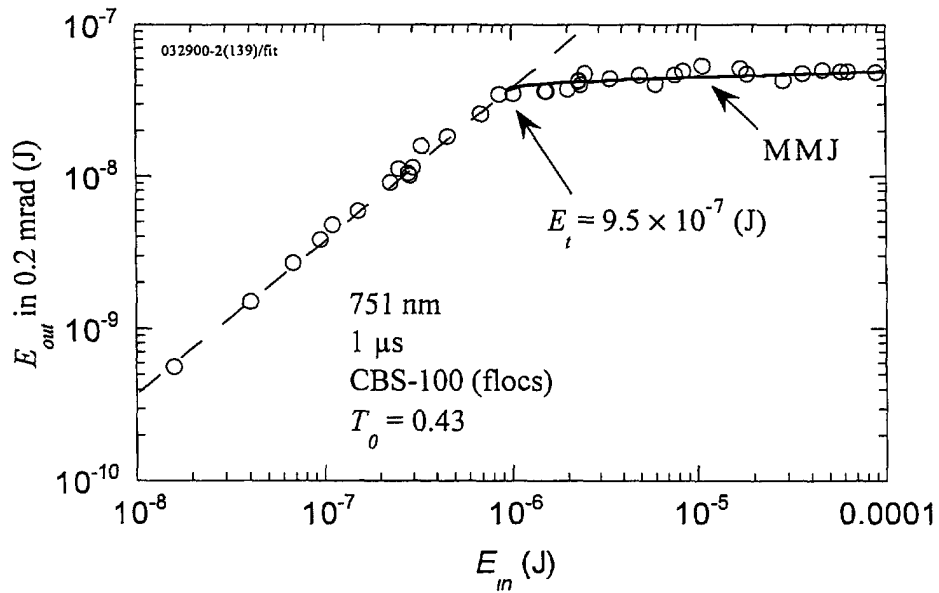


Figure 15. Threshold determination in a sample of CBS-100 (flocs) for long pulses: MMJ fit

UNCLASSIFIED

Distribution list

INTERNAL DISTRIBUTION

DREV TR – 2001-028

1 - Deputy Director General
1 - Chief Scientist
6 - Document Library
1 - D. Vincent (author)
1 - A. Cantin
1 - G. Otis
1 - J.-M. Garneau
1 - J. Dubois
1 - L. Bissonnette
1 - J.-M. Thériault
1 - G. Roy
1 - R. Durand
1 - G. Fournier
1 - J. Cruickshank
1 - P. Mathieu
1 - V. Larochelle
1 - J.-R. Simard

EXTERNAL DISTRIBUTION

DREV TR – 2001-028

- 1 - DRDKIM
- 1 - DRDKIM (unbound copy)
- 1 - DRDC
- 1 - DREO
- 1 - DREA
- 1 - DRES
- 1 - DCIEM
- 1 - DSTL
- 1 - DSTM
- 1 - DSTA
- 1 - DSTHP
- 1 – J2 STI
- 1 - Defence Evaluation and Research Agency
 - St. Andrews Road
 - Malvern
 - Worcester, WR14 3PS
 - United Kingdom
 - Attn: Dr. R.C. Hollins

UNCLASSIFIED
 SECURITY CLASSIFICATION OF FORM
 (Highest Classification of Title, Abstract, Keywords)

DOCUMENT CONTROL DATA		
1 ORIGINATOR (name and address) Defence Research Establishment Valcartier	2 SECURITY CLASSIFICATION (Including special warning terms if applicable) UNCLASSIFIED	
3. TITLE (Its classification should be indicated by the appropriate abbreviation (S, C, R or U)) Measurement of Optical Limiting Threshold in Various Materials		
4. AUTHORS (Last name, first name, middle initial If military, show rank, e.g. Doe, Maj John E.) Denis Vincent		
5 DATE OF PUBLICATION (month and year) October 2001	6a NO. OF PAGES 36	6b .NO OF REFERENCES 15
7 DESCRIPTIVE NOTES (the category of the document, e.g technical report, technical note or memorandum Give the inclusive dates when a specific reporting period is covered) Technical report		
8. SPONSORING ACTIVITY (name and address) N/A		
9a PROJECT OR GRANT NO. (Please specify whether project or grant) 2km	9b. CONTRACT NO	
10a ORIGINATOR'S DOCUMENT NUMBER TR 2001-028	10b OTHER DOCUMENT NOS N/A	
11 DOCUMENT AVAILABILITY (any limitations on further dissemination of the document, other than those imposed by security classification)		
<input checked="" type="checkbox"/> Unlimited distribution <input type="checkbox"/> Contractors in approved countries (specify) <input type="checkbox"/> Canadian contractors (with need-to-know) <input type="checkbox"/> Government (with need-to-know) <input type="checkbox"/> Defense departments		
12 DOCUMENT ANNOUNCEMENT (any limitation to the bibliographic announcement of this document This will normally correspond to the Document Availability (11). However, where further distribution (beyond the audience specified in 11) is possible, a wider announcement audience may be selected.) As in item 11		

UNCLASSIFIED
 SECURITY CLASSIFICATION OF FORM
 (Highest Classification of Title, Abstract, Keywords)

UNCLASSIFIED
 SECURITY CLASSIFICATION OF FORM
 (Highest Classification of Title, Abstract, Keywords)

13. ABSTRACT (a brief and factual summary of the document. It may also appear elsewhere in the body of the document itself. It is highly desirable that the abstract of classified documents be unclassified. Each paragraph of the abstract shall begin with an indication of the security classification of the information in the paragraph (unless the document itself is unclassified) represented as (S), (C), (R), or (U). It is not necessary to include here abstracts in both official languages unless the text is bilingual)

In the search for materials suitable for optical limiting applications to protect eyes and electro-optical sensors against laser radiation, fine carbon particles suspended in a liquid have been shown to possess highly desirable properties. This publication reports on the measurement of the threshold energy fluence for optical limiting of nanosecond and microsecond pulses in a high-performance carbon suspension named DREV CBS-100. Thresholds as low as 24 mJ/cm^2 (nanosecond regime) and 100 mJ/cm^2 (microsecond regime) have been obtained. The technique has been tested by measuring materials whose properties can be found in the technical literature.

14. KEYWORDS, DESCRIPTORS or IDENTIFIERS (technically meaningful terms or short phrases that characterize a document and could be helpful in cataloguing the document. They should be selected so that no security classification is required. Identifiers, such as equipment model designation, trade name, military project code name, geographic location may also be included. If possible keywords should be selected from a published thesaurus, e.g. Thesaurus of Engineering and Scientific Terms (TEST) and that thesaurus-identified. If it is not possible to select indexing terms which are Unclassified, the classification of each should be indicated as with the title)

Optical Limiters
 Limiting Threshold
 Carbon Suspensions
 CBS-100
 RSA Materials
 Nd YAG Laser

516302
 CA011743

UNCLASSIFIED
 SECURITY CLASSIFICATION OF FORM
 (Highest Classification of Title, Abstract, Keywords)